



The Compact Muon Solenoid Experiment  
**Conference Report**

Mailing address: CMS CERN, CH-1211 GENEVA 23, Switzerland



27 January 2020 (v3, 09 August 2021)

# The CT-PPS tracking system performance in LHC-Run2 and prospects for LHC-Run3

Maria Margherita Obertino for the CMS Collaboration

## Abstract

The CT-PPS (CMS TOTEM Precision Proton Spectrometer, now PPS) system consists of tracking and timing detectors installed along the LHC beam line between 210 and 220 m from the interaction point on both sides of the CMS experiment. The aim of the apparatus is to measure with high precision the position, direction and time-of-flight of protons which emerge intact from the pp collision. Fully integrated in the CMS data acquisition system, PPS has taken data at high luminosity during the years of the LHC-Run2 (2016-2018), with slightly different detector configurations. The tracking system consists of 4 detector stations (two per side) and was instrumented with edgeless silicon strips (2016-2017) and 3D pixel sensors bump-bonded to the PSI46dig ROC (2017-2018). In this contribution commissioning, operation and performance of the CT-PPS tracking system during Run2 will be discussed, with focus on the challenges posed by the fact that detectors were operated at few millimeters from the beam, in highly non-uniform irradiation environment. Prospects for LHC-Run3 will be also presented.

Presented at *IPRD2019 15th Topical Seminar on Innovative Particle and Radiation Detectors*. Published in <https://doi.org/10.1088/1748-0221/15/05/C05049>

# The PPS tracking system: performance in LHC Run2 and prospects for LHC Run3

To cite this article: M.M. Obertino 2020 *JINST* **15** C05049

View the [article online](#) for updates and enhancements.

## Recent citations

- [Intrinsic time resolution of 3D-trench silicon pixels for charged particle detection](#)  
L. Anderlini *et al*



**IOP | ebooks™**

Bringing together innovative digital publishing with leading authors from the global scientific community.

Start exploring the collection—download the first chapter of every title for free.

15<sup>TH</sup> TOPICAL SEMINAR ON INNOVATIVE PARTICLE AND RADIATION DETECTORS  
14–17 OCTOBER 2019  
SIENA, ITALY

## The PPS tracking system: performance in LHC Run2 and prospects for LHC Run3

**M.M. Obertino on behalf of CMS and TOTEM collaborations**

*Dipartimento di Scienze Agrarie, Forestali ed Alimentari, Università di Torino,  
Largo Paolo Braccini 2, Grugliasco TO, Italy*

*INFN — Sezione di Torino,  
via Pietro Giuria 1, 10125, Turin, Italy*

*E-mail: [margherita.obertino@cern.ch](mailto:margherita.obertino@cern.ch)*

**ABSTRACT:** The PPS (Precision Proton Spectrometer) system consists of tracking and timing detectors installed along the LHC beam line between 210 and 220 m from the interaction point on both sides of the CMS experiment. The aim of the apparatus is to measure with high precision the position, direction and time-of-flight of protons which emerge intact from the pp collision. Fully integrated in the CMS data acquisition system, PPS has taken data at high luminosity during the years of the LHC Run2 (2016–2018), with slightly different detector configurations. The tracking system consists of 4 detector stations (two per side) and was instrumented with edgeless silicon strips (2016–2017) and 3D pixel sensors bump-bonded to the PSI46dig ROC (2017–2018). In this contribution, commissioning, operation and performance of the PPS tracking system during Run2 will be discussed, with focus on the challenges posed by operating the detectors at few millimeters from the beam, in highly non-uniform irradiation environment. Prospects for LHC Run3 will be also presented.

**KEYWORDS:** Particle tracking detectors; Particle tracking detectors (Solid-state detectors); Pixelated detectors and associated VLSI electronics; Radiation-hard detectors

---

## Contents

<b>1</b>	<b>Introduction</b>	<b>1</b>
<b>2</b>	<b>The PPS tracking system</b>	<b>2</b>
2.1	Strip detectors	4
2.2	Pixel detectors	4
<b>3</b>	<b>Tracking detector efficiency</b>	<b>5</b>
3.1	Silicon strip detector efficiency	5
3.2	3D pixel detector efficiency	6
<b>4</b>	<b>Prospect for LHC Run3</b>	<b>7</b>
<b>5</b>	<b>Conclusions</b>	<b>8</b>

---

## 1 Introduction

Born in 2014 as a joint project of the CMS [1] and TOTEM [2] Collaborations, PPS (Precision Proton Spectrometer) [3] is a CMS subdetector designed to study central exclusive production (CEP) in proton-proton collisions at the Large Hadron Collider (LHC) in standard high-luminosity running conditions. In CEP processes,  $pp \rightarrow pXp$ , protons interact via photon or colour singlet exchanges to produce centrally a system X, which may be a particle or a more complex object. The peculiarity of these events is that both protons emerge intact from the collision, having lost a fraction of their momentum so small that they do not leave the vacuum beam pipe. This creates a very distinct experimental signature, i.e. the presence of two protons, scattered at very small angle on opposite sides of the interaction point, whose kinematics perfectly matches that of the system X. CEP provides a unique method to search for and characterize new heavy particles in particularly clean experimental conditions, thanks to the absence of proton remnants. Moreover, specific CEP processes allow to look for deviations from the Standard Model predictions, which would reveal a sign of new physics (e.g. diboson production to search for anomalous quartic gauge couplings [4]).

CEP events are reconstructed with the CMS apparatus by using the central detector to measure the system X and PPS to tag the two leading protons and measure their momentum. PPS is a magnetic spectrometer made of tracking and timing detectors installed along the LHC beam line at about 220 m from the CMS interaction point (IP5). The LHC magnets between IP5 and the detector stations are used to bend out of the beam envelope the two leading protons, making their detection possible [3]. The tracking system measures the position and direction of the protons, which in turn allows the reconstruction of the mass and momentum of the centrally produced system X (i.e.  $M_X = \sqrt{\xi_1 \xi_2 s}$ , with  $\xi$  fractional momentum loss of the proton and  $\sqrt{s}$  the pp centre of mass energy). The detectable mass ( $M_X$ ) depends on the optics in the accelerator and ranges between

300 GeV and 1800 GeV. The  $\xi$  resolution is in the range 0.5–3%, depending on  $\xi$  itself [3]. Timing detectors measure the time-of-flight of the protons, allowing to identify the CEP interaction vertex (z-by-timing technique) and, consequently, reducing the background from multiple proton-proton collisions, i.e. pile-up events (PU). To maximize acceptance for low momentum-loss protons, detectors must operate at distances of few mm from the beam centre, without affecting LHC operation. To achieve this, all PPS detectors are installed in secondary vacuum vessels, called Roman Pots (RP) [2], and moved into the primary vacuum of the LHC through vacuum bellows. The Roman Pot system allows to insert safely detectors up to 1.5 mm from the beam axis during data taking and to move them away from the beam during injection and acceleration.

A schematic layout of the LHC beam line between IP5 and the location of PPS Roman Pots on one of the two sides of CMS (LHC sector 56) is shown in figure 1. A similar structure, but symmetric with respect to the CMS interaction point, is present in LHC sector 45. Each sector hosts three RP stations: two, located at  $\sim 210$  m (210 FAR) and  $\sim 220$  m (220 FAR) from IP5, are equipped with tracking detectors; one, located at  $\sim 215$  m from IP5, houses the timing detectors.

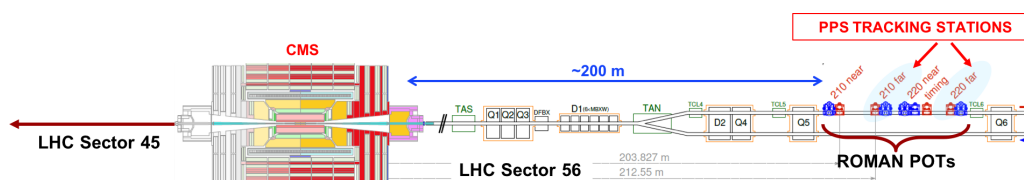


**Figure 1.** Schematic layout of the LHC beam line between the CMS interaction point and the location of PPS Roman Pots for LHC sector 56. The same structure, symmetric with respect to CMS, is present in LHC sector 45. The PPS RPs are shown in red; those in blue are part of the TOTEM apparatus and are used by PPS only during special alignment runs taken at the beginning of a data taking period to precisely measure the position of the detectors with respect to the beam centre. The position of LHC dipoles (Dn), quadrupoles (Qn) and target absorbers (TAN,TAS) is also shown.

PPS successfully took data integrated in CMS during LHC Run2 (2016–2018) with different detector configurations. In the following sections, the PPS tracking system and its performance during LHC Run 2 will be discussed. Characteristics and performance of the PPS timing detectors are described in [5].

## 2 The PPS tracking system

The PPS tracking system allows to measure the position and direction of protons that have lost in the collision a fraction of their momenta approximately between 2% and 20%. The following requirements were taken into account while designing the detector:

- a position resolution of  $\sim 10 \mu\text{m}$  per station and an angular resolution of few  $\mu\text{rad}$  are needed to reach the target resolution of  $2 \text{ GeV}/c^2$  on the mass of the centrally produced system X;
- a minimal insensitive area at the detector edge facing the beam is necessary to maximize the acceptance for low- $\xi$  protons;
- because of the small distance from the LHC beam at which detectors have to operate, tolerance to an high level of non uniform irradiation is mandatory; for a collected integrated luminosity

of  $100 \text{ fb}^{-1}$  the expected proton flux in the region closest to the beam is  $5 \times 10^{15} \text{ p/cm}^2$ , which corresponds to a fluence between 1 and  $3 \times 10^{15} \text{ n}_{\text{eq}}/\text{cm}^2$ ;

- detectors with multi-track capability are necessary to maximize the tracking efficiency; in high pile-up conditions, more than 20% of the events recorded have more than one track in each Roman Pot station.

Taking all the requirements into account, 3D silicon pixel sensors [6] were chosen as baseline solution for the PPS tracking system.

The start of the PPS program, initially foreseen for 2017, was moved up to 2016. Since the silicon pixel sensors were not ready, the two tracking stations were instrumented with the TOTEM silicon strips [2]. Even if these detectors were not optimal because of their limited radiation hardness and low efficiency in a multi-track environment, this allowed to demonstrate one year in advance the feasibility to operate detectors close to the beam-line at high luminosity. Moreover, the study of the  $pp \rightarrow pl^+l^-p$  processes performed on the data collected in 2016 brought to the first observation of (semi)exclusive  $\gamma\gamma$  collisions at the electroweak scale [7]. 3D silicon detectors were installed in the two stations at 220 m in 2017; the design configuration with all stations instrumented with pixels was finally met in 2018.

Figure 2 shows the strip (left) and 3D pixel (right) detector packages. Each package is installed inside a Roman Pot, in the secondary vacuum ( $p < 20 \text{ mbar}$ ). Glued to the flange which separates the vacuum chamber containing the detector and the atmosphere, there is the so-called Motherboard (MB), a custom designed card which distributes the bias voltage to each sensor individually, provides the low voltage and allows to configure the read-out chips (ROCs), receives data from the detectors, performs the electrical to optical signal conversion and transfers data to the Data Acquisition System (DAQ). The MB also hosts the radiation and temperature monitoring sensors. In figure 2 are also visible the cooling capillary tubes. The evaporative cooling system based on  $\text{C}_3\text{F}_8$  developed for the TOTEM experiment [2] was used to keep the temperature at  $-10^\circ$  inside the strip RP and at  $-20^\circ$  inside the pixel RP, to reduce the increase of the leakage current induced by radiation.

The PPS tracking system was operated regularly during the LHC Run2. About  $115 \text{ fb}^{-1}$  of data were collected with the tracking Roman Pots inserted, corresponding for 2017–2018 to 90% of the data recorded by CMS.

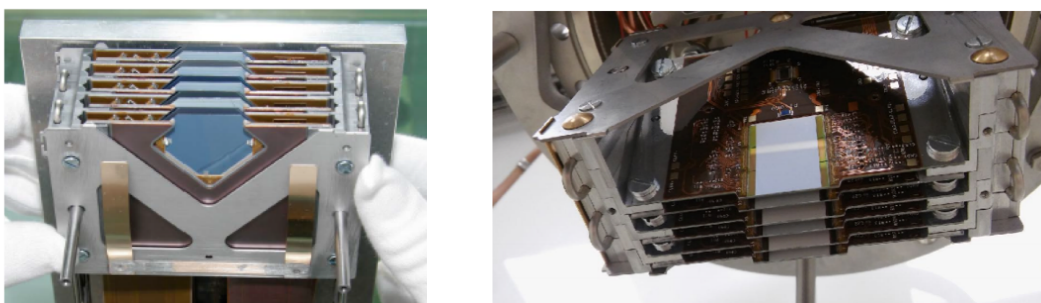


**Figure 2.** PPS strip (left) and pixel (right) detector packages.

## 2.1 Strip detectors

A strip detector package (figure 2 left) consists of a stack of 5 “double-planes” of 300  $\mu\text{m}$  thick strip sensors implemented on a very high resistivity n-type silicon wafer. Each plane contains 512  $\text{p}^+$  strips with 66  $\mu\text{m}$  pitch. To allow the reconstruction of the two impact point coordinates (x,y), two planes with strips mounted with orthogonal orientations are placed back-to-back, forming a “double-plane”. The insensitive area at the edge of the sensor facing the beam was reduced to 50  $\mu\text{m}$  by implementing Current Terminated Structures (CTS), rings which surround the active area of the sensor and collect the high current generated in the diced edge. The strips of each plane are binary read out by 4 VFAT2 chips [8]. The silicon sensor and the 4 ROCs are located on a flexible circuit which is connected to the strip Motherboard. The same back-end electronics used by the TOTEM experiment has been adopted.

This detector has been designed to run in low-luminosity and low-PU conditions. It guarantees a very good track resolution (10  $\mu\text{m}$  for both the reconstructed coordinates) but has limitations in reconstructing events with multiple tracks. Moreover, irradiation studies showed that sensors are capable of withstanding a dose up to  $10^{14}$   $\text{n}_{\text{eq}}/\text{cm}^2$ , corresponding to few  $\text{fb}^{-1}$  of data collected at LHC.

## 2.2 Pixel detectors

A pixel detector package consists of 6 planes of 3D silicon sensors read-out by PSI46dig ROCs [9]. Planes are tilted inside the Roman Pot by  $18.4^\circ$  to increase the charge sharing and improve the resolution.

3D sensors were chosen for their intrinsic radiation hardness and for the possibility to implement slim edges. The sensors used by PPS were produced by CNM (Barcelona, Spain) through a double-sided process, with non-passing-through columns. This design allows to reach easily the  $\text{p}^+$  bias electrodes, where a negative voltage is applied, while the side where the  $\text{n}^+$  columns are etched is bump-bonded to the ROC. Sensors were built on a 230  $\mu\text{m}$  thick wafer; columns are 200  $\mu\text{m}$  deep and have a diameter of 10  $\mu\text{m}$ . The pixel size, compatible with the chosen ROC, is  $100 \times 150 \mu\text{m}^2$ . Two pixel configurations were used, with one (1E) and two (2E) readout columns. A 200  $\mu\text{m}$  slim edge was implemented with a triple p-type column fence surrounding the sensitive area. Due to problems occurred during the production, not all the sensors used in PPS had the initially foreseen size which corresponds to a matrix of  $3 \times 2$  ROCs; part of them had a size corresponding to a matrix of  $2 \times 2$  ROCs (in the following referred to as “ $2 \times 2$  sensors”).

Every PPS 3D pixel sensor is glued to the support plate and wire-bonded to the so-called “RPix flex hybrid”, a 4-layer circuit printed on a flexible kapton support, which distributes power, clock and trigger to the ROCs and the bias voltage to the sensor. One Token Bit Manager (TBM) chip per flex reads out the six PSI46dig ROCs of the module using a token ring protocol and serializes the data over a single output line. Front-end boards for data (FED) and control (FEC) are the same used for the CMS Phase I pixel tracker upgrade [10]. The connection between detectors and front-end electronics is guaranteed by the RPix Motherboard, a card with a structure similar to the one used for the strip, but customized to be compatible with the CMS pixel read-out.

The suitability of 3D sensors for PPS was confirmed by the results obtained in several beam tests and irradiation campaigns [11]. A resolution of 22  $\mu\text{m}$  (25  $\mu\text{m}$ ) for 2E (1E) sensors and a



global efficiency greater than 99.5% for unirradiated sensors tilted by more than  $5^\circ$  with respect to the beam axis were measured. Detectors were fully calibrated and optimized by means of the internal calibration circuit of the ROC. The read-out threshold was set to  $\sim 2000 e^-$  at the beginning of the data taking, with a spread among pixels of the order of  $150 e^-$ . The fraction of dead or noisy channels was less than 0.1% during the whole LHC Run2 data taking period.

### 3 Tracking detector efficiency

The efficiency of the strip and pixel detectors was continuously monitored during the data taking in order to check its evolution due to radiation damage. In the following sections, final results obtained in 2017 and 2108 are shown. The LHC data taking was stopped three times for about one week in both 2017 and 2018 to allow maintenance work for the accelerator and the experiments (technical stops, TS). PPS took advantage of these periods to perform actions finalized to recover, at least partially, the inefficiency caused by radiation.

Other reconstruction effects, such as those due to showers within the detector material, are not covered here; their contribution to the efficiency for finding proton tracks has been estimated to be of the order of few percent.

#### 3.1 Silicon strip detector efficiency

The two major sources of inefficiency for the PPS strip detector, i.e. irradiation and the presence of multiple tracks in the event, were studied separately.

The inefficiency due to multiple tracks was evaluated for each RP separately and for different data taking periods [12]. Figure 3 shows the efficiency versus pile-up obtained for detectors installed in LHC sector 45 using data collected in October and November 2017. This efficiency is inversely related to the PU, as expected, and ranges between 40% and 80%. Similar results were obtained for the other data taking periods and for LHC sector 56 detectors.

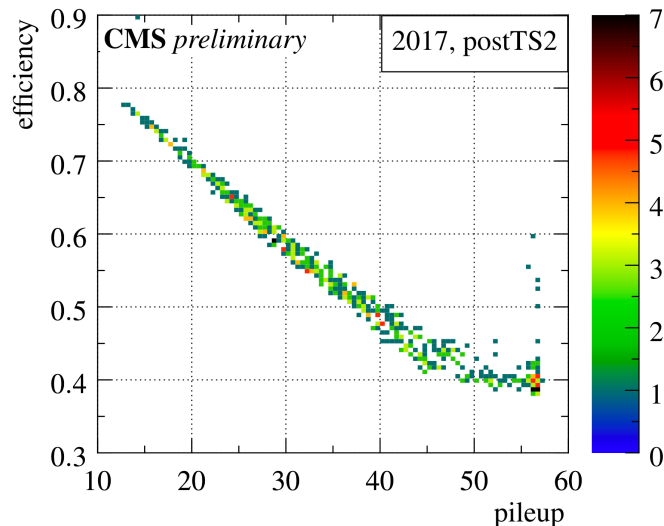


**Figure 3.** Strip efficiency versus pile-up for the data taking period between the second and the third 2017 TS (October–November).



The time-dependent effects of radiation on the strip detector efficiency have been studied selecting events with exactly 1 track reconstructed in the pixel detector; strip tracks were required to match the reference pixel track within  $|\Delta\xi| < 0.01$  to be counted as efficient [13].

Figure 4 shows the strip efficiency maps produced with the first data collected in 2017 ( $L_{\text{INT}} \sim 2.4 \text{ fb}^{-1}$ ) for the region covered by the pixel detector acceptance, and below the collimator aperture limits (region relevant for physics). The area damaged by radiation is clearly visible, especially for detectors in LHC sector 45. The size and inefficiency of the most affected area grow with integrated luminosity during the data taking. To mitigate this effect the sensor bias voltage was raised several times and detectors were replaced with a set of spares during the second 2017 technical stop.

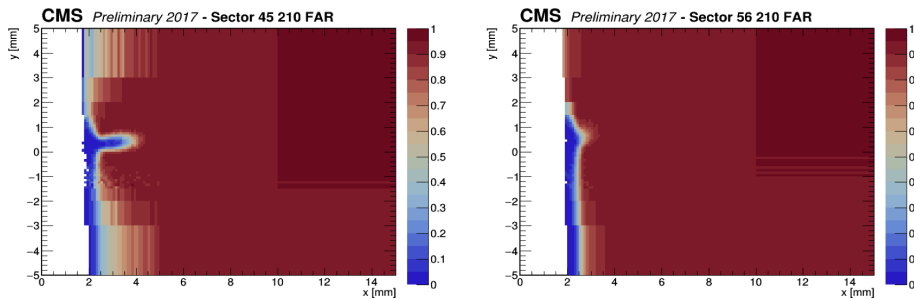


**Figure 4.** RP tracking efficiency maps produced with the first data collected in 2017 for the strip detector in sector 45 (left) and 56 (right). The radiation damaged area is clearly visible on the left edge of the sensor.

### 3.2 3D pixel detector efficiency

A track is reconstructed in a PPS pixel station by fitting hits in at least 3 out of the 6 planes that form a detector package. The efficiency of each station was determined as a function of the transverse coordinates  $(x,y)$  with a two-step procedure [14]. First of all, the efficiency of every pixel in each plane was evaluated; then, these values were used to calculate the tracking station efficiency as the probability of having at least three efficient pixels out of six. Figure 5 shows the efficiency map at the beginning of 2017 data taking (similar results were obtained in 2018). The efficiency is well above 99% everywhere, except for the area not covered by the “ $2 \times 2$  sensor” present in each station.

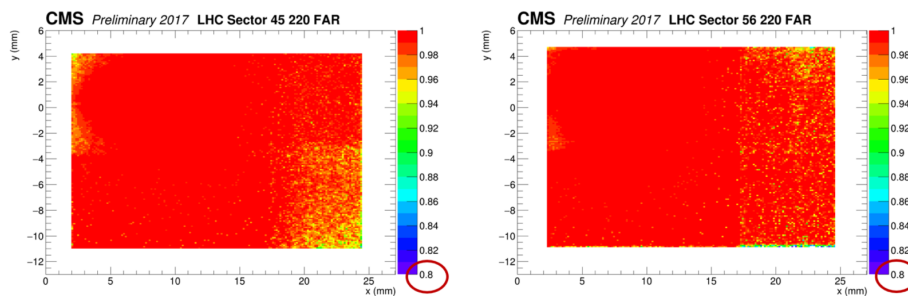


**Figure 5.** RP tracking efficiency maps obtained at the beginning of the 2017 data taking period for the pixel detectors installed in LHC sector 45 (left) and 56 (right). The efficiency is well above 99% everywhere, except for the area above  $x \simeq 17$  mm, covered by 5 planes instead of 6.

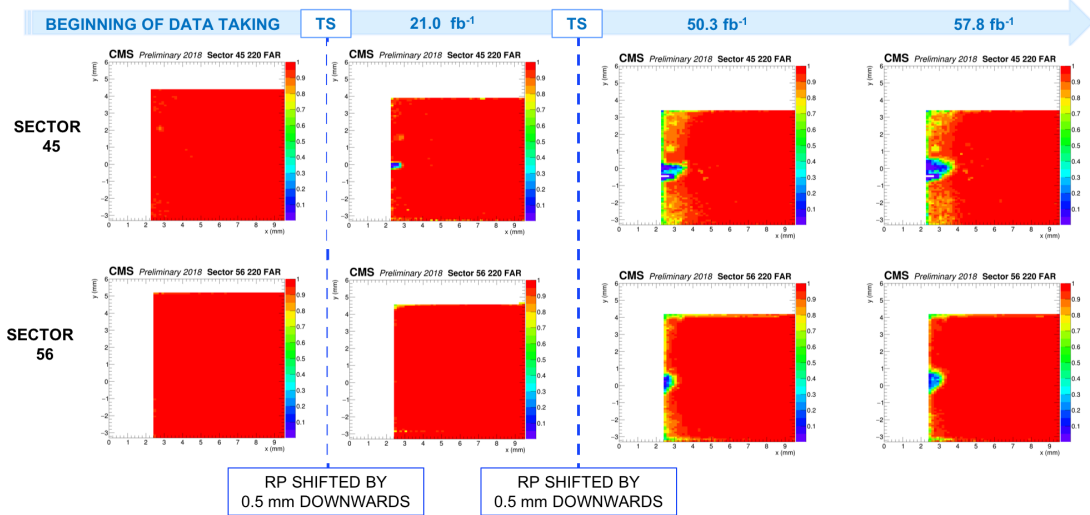


**Figure 6.** Evolution of the RP tracking efficiency map in the pixel detector region closest to the beam for LHC sector 45 (top row) and 56 (bottom row) during 2018 data taking period. RPs were shifted downwards twice, during the first two technical stops (TS). The small spot of white bins ( $y \sim -0.4$  mm,  $x < 2.8$  mm) within the LHC Sector 45 220 FAR damage is a cluster of a few dead pixels.

A decrease of the efficiency in time due to radiation was observed. This effect is mainly due to the ROC, the design of which is not optimized to operate in non-uniform irradiation. In these conditions, the analog current supplied to the most and to the least irradiated pixel units is different. As a consequence, the output signals from the most irradiated pixels slow down and, if the difference in irradiation among the pixels of the same ROC is high, it becomes impossible to read all of them in the same bunch crossing window, making the module inefficient. Figure 6 shows the evolution of the RP efficiency map in the detector region closest to the beam during the 2018 data taking period. In the first two technical stops, the whole detector was shifted by 0.5 mm vertically to displace the most exposed spot and thus extend the detector lifetime. As a consequence, the vertical width of the damaged region increases as a function of the integrated luminosity. Figure 6 also shows that detectors in LHC sector 56 suffered a smaller radiation damage. This is due to the different irradiation profile caused by differences in the optical functions of the two sectors.

The left plot of figure 7 shows the average efficiency as a function of the integrated luminosity in the critical region around the irradiation peak (right plot in the same figure). The drop in the efficiency due to irradiation and the recovery after each TS are clearly visible for all the tracking stations. The average efficiency in the area surrounding the critical region remained high ( $\sim 99\%$ ) and constant during the whole data taking.

#### 4 Prospect for LHC Run3

PPS will take data during LHC Run3 starting in 2021. The apparatus will consist of 2 tracking stations and 2 timing stations per LHC sector. The tracking RP will be equipped with 3D silicon pixel sensors read out by the PROC600 chips [15] currently used in the first layer of the CMS central pixel detector. New sensors 150  $\mu\text{m}$  thick are being produced by FBK in single-sided technology. One sensor size ( $2 \times 2$ ) and one electrode configuration (2E) has been chosen.

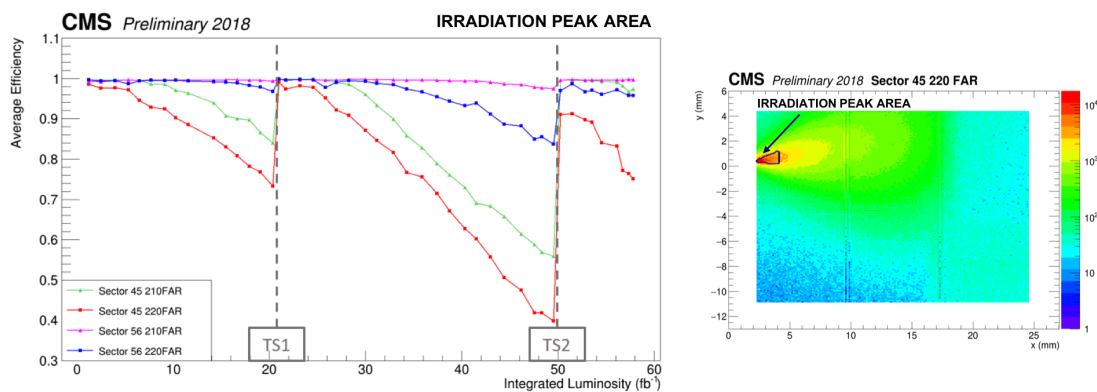


**Figure 7.** Average RP tracking efficiency as a function of the integrated luminosity in the critical region around the irradiation peak (left plot). The irradiation peak area is shown superimposed to the hit map in the right plot. The drop in the efficiency due to irradiation and the recovery after each LHC technical stop (TS) due to vertical movement of the RPs, are clearly visible.

Irradiation tests performed on the PROC600 show a behaviour similar to the PSI46dig. To mitigate the effect of radiation on the efficiency every detector package will be equipped with a piezo-electric motor that will make possible finer, remotely controlled, vertical movements. This should allow to better distribute the radiation damage with respect to LHC Run2 and to reduce its impact. The plot shown in figure 7 will be produced in real time to define when detectors need to be shifted.

## 5 Conclusions

The PPS tracking system has been successfully operated since the beginning of LHC Run2 with overall very good performance, high efficiency and tracking capability despite the high and non uniform irradiation conditions. Data corresponding to more than  $100 \text{ fb}^{-1}$  have been collected with the tracking Roman Pots inserted; studies of several (semi)exclusive processes are ongoing. PPS will continue its program in LHC Run3 with the goal of reaching a total integrated luminosity of  $\sim 300 \text{ fb}^{-1}$ . New 3D silicon pixel sensors read-out by the PROC600 chip will be installed in the 4 tracking stations. A remotely controlled movement system will allow to shift the detector packages in order to contain the efficiency degradation due to irradiation.

## References

- [1] CMS collaboration, *The CMS experiment at the CERN LHC*, 2008 *JINST* **3** S08004.
- [2] TOTEM collaboration, *The TOTEM experiment at the CERN Large Hadron Collider*, 2008 *JINST* **3** S08007.
- [3] CMS and TOTEM collaborations, *CMS-TOTEM Precision Proton Spectrometer*, CERN-LHCC-2014-021 (2014).
- [4] T. Pierzchała and K. Piotrkowski, *Sensitivity to anomalous quartic gauge couplings in photon-photon interactions at the LHC*, *Nucl. Phys. Proc. Suppl.* **257** (2008) 179 [arXiv:0807.1121].

- [5] E. Bossini, *The CMS Precision Proton Spectrometer timing system performance in Run 2, future upgrades and sensor radiation hardness studies*, talk given at the 15<sup>th</sup> Topical Seminar on Innovative Particle and Radiation Detectors, October 14–17, Siena, Italy (2019).
- [6] S. Parker et al., *3D — A proposed new architecture for solid-state radiation detectors*, *Nucl. Instrum. Meth. A* **395** (1997) 328.
- [7] CMS and TOTEM collaborations, *Observation of proton-tagged, central (semi)exclusive production of high-mass lepton pairs in pp collisions at 13 TeV with the CMS-TOTEM precision proton spectrometer*, *JHEP* **07** (2018) 153 [[arXiv:1803.0449](#)].
- [8] P. Aspell et al., *VFAT2: a front-end system on chip providing fast trigger information, digitized data storage and formatting for charge readout of multi-channel silicon and gas particle detectors*, *Electronics for particle physics*, talk given at *Topical Workshop on Electronics for Particle Physics (TWEPP 2007)*, September 3–7, Prague, Czech Republic (2007).
- [9] H.C. Kastli, *Frontend electronics development for the CMS pixel detector upgrade*, *Nucl. Instrum. Meth. A* **731** (2013) 88.
- [10] A. Dominguez et al., *CMS technical design report for the pixel detector upgrade*, [CERN-LHCC-2012-016](#) (2012).
- [11] F. Ravera, *3D silicon pixel detectors for the CT-PPS tracking system*, Ph.D. thesis, Torino University, Turin Italy (2016).
- [12] CMS and TOTEM collaborations, *Efficiency of Si-strips sensors used in Precision Proton Spectrometer*, [CERN-CMS-DP-2018-056](#) (2018).
- [13] CMS collaboration, *Efficiency of the Si-strips sensors used in Precision Proton Spectrometer: radiation damage*, [CERN-CMS-DP-2019-035](#) (2019).
- [14] CMS collaboration, *Efficiency of the Pixel sensors used in the Precision Proton Spectrometer: radiation damage*, [CERN-CMS-DP-2019-036](#) (2019).
- [15] CMS Collaboration, *High rate capability and radiation tolerance of the new CMS pixel detector readout chip PROC600*, [2017 JINST 12 C01078](#).